Direct estimation of the seismic demand and capacity of MDOF systems through Incremental Dynamic Analysis of an SDOF approximation[1]

Dimitrios Vamvatsikos[2] and C. Allin Cornell, M.ASCE[3]

Abstract: Introducing a fast and accurate method to estimate the seismic demand and capacity of first-mode-dominated multi-degree-of-freedom systems in regions ranging from near-elastic to global collapse. This is made possible by exploiting the connection between the Static Pushover (SPO) and the Incremental Dynamic Analysis (IDA). While the computer-intensive IDA would require several nonlinear dynamic analyses under multiple suitably-scaled ground motion records, the simpler SPO helps approximate the multi-degree-of-freedom system with a single-degree-of-freedom oscillator whose backbone matches the structure's SPO curve far beyond its peak. Similar methodologies exist but they usually employ oscillators with a bilinear backbone. In contrast, the empirical equations implemented in the SPO2IDA software allow the use of a complex quadrilinear backbone shape. Thus, the entire summarized IDA curves of the resulting system are effortlessly generated, enabling an engineer-user to obtain accurate estimates of seismic demands and capacities for limit-states such as immediate occupancy or global dynamic instability. Using three multistory buildings as case studies, the methodology is favorably compared to the full IDA.

CE Database keywords: Nonlinear analysis; Static analysis; Dynamic analysis; Seismic response; Earthquakes; Performance evaluation; Buildings, multistory; Approximation methods.

Introduction

At the core of Performance-Based Earthquake Engineering (PBEE) lies the accurate estimation of the seismic demand and capacity of structures, a task that several methods are being proposed to tackle. One of the promising candidates is Incremental Dynamic Analysis (IDA) (Vamvatsikos and Cornell, 2002), a computer-intensive procedure that has been incorporated in modern seismic codes (e.g., Federal Emergency Management Agency, FEMA, 2000) and offers thorough demand and capacity prediction capability, in regions ranging from elasticity to global dynamic instability, by using a series of nonlinear dynamic analyses under suitably multiply-scaled ground motion records. Still, professional practice favors simplified methods, mostly using single-degree-of-freedom (SDOF) models that approximate the multi-degree-of-freedom (MDOF) system's behavior by matching its Static Pushover (SPO) curve, coupled with empirical equations derived for such oscillators to rapidly obtain a measure of the seismic demand (e.g., Fajfar and Fischinger, 1988; Fajfar and Gaspersic, 1996; FEMA, 1997). Such procedures could be extended to reach far into the nonlinear range and approximate the results of IDA, but they use oscillators with bilinear backbones that only allow for elastic perfectly-plastic behavior, and occasionally positive or negative post-yield stiffness (e.g., Miranda, 2000;

[1]Based on a short paper presented at the 5th European Conference on Structural Dynamics EURODYN 2002, Munich, Germany, 2002

[2]Researcher, Dept. of Mechanical and Industrial Engineering, Univ. of Thessaly, Volos, Greece

[3]Professor, Dept. of Civil and Environmental Engineering, Stanford Univ., Stanford, CA 94305-4020

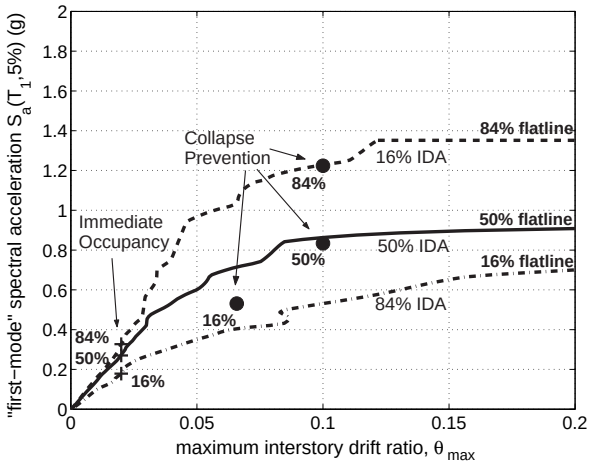

Fig. 1. The 16%, 50%, 84% fractile IDAs and limit-state capacities.

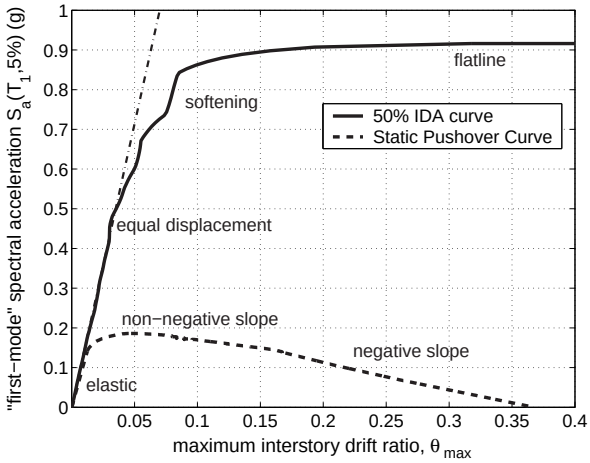

Fig. 2. The median IDA compared against the SPO generated by an inverted-triangle load pattern.

Nassar and Krawinkler, 1991; Al-Sulaimani and Roessett, 1985). With the emergence of the SPO2IDA software (Vamvatsikos and Cornell, 2004b), empirical relations for full quadrilinear backbones are readily available, which, when suitably applied to the MDOF SPO, provide the ability to accurately approximate the full IDA and investigate the connection between the structure's SPO curve and its seismic behavior.

IDA fundamentals

IDA (Vamvatsikos and Cornell, 2002) involves performing a series of nonlinear dynamic analyses of a structural model for multiple records by scaling each record to several levels of intensity that are suitably selected to uncover the full range of the model's behavior: from elastic to yielding and nonlinear inelastic, finally leading to global dynamic instability. Each dynamic analysis can be characterized by at least two scalars, an Intensity Measure (*IM*), which represents the scaling factor of the record (e.g., the 5%-damped first-mode spectral acceleration $S_a(T_1,5\%)$) and an Engineering Demand Parameter (*EDP*), which monitors the structural response of the model (e.g., maximum, over all stories, peak interstory drift ratio $\theta_{\max}$ or peak roof drift ratio θ_{roof}). Note that previously (e.g., Vamvatsikos and Cornell, 2002), the term Damage Measure *DM* was used instead of *EDP* but the latter is now preferred as it corresponds to the current terminology of the Pacific Earthquake Engineering Research (PEER) Center.

To illustrate the proposed methodology, IDA will be performed for a centerline model of a 9-story steel moment-resisting frame designed for Los Angeles according to the 1997 National Earthquake Hazards Reduction Program (NEHRP) provisions (Lee and Foutch, 2002). The model incorporates ductile members, shear panels and realistically fracturing Reduced Beam Section connections, while it includes the influence of interior gravity columns and a first-order treatment of global geometric nonlinearities (P-Δ effects). Essentially, it is a first-mode-dominated structure that has its fundamental mode at a period of $T_1 = 2.3$ s, accounting for 84.3% of the total mass, hence allowing for some significant sensitivity to higher modes. Additionally, a suite of twenty ground motion records has been compiled to represent a scenario earthquake (Vamvatsikos and Cornell, 2004a); the moment magnitude is within the range of 6.5 – 6.9, they have all been recorded on firm soil and show no directivity effects.

Having performed the required dynamic analyses and by suitably interpolating between the *IM* and *EDP* results, an IDA curve can be plotted for each record on the *EDP*-*IM* axes. If

stripes of *EDP*-values are calculated at several levels of the *IM* and the 16%, 50% and 84% fractile *EDP*-values given the *IM*-level are estimated, the twenty IDA curves can be summarized into 16%, 50% and 84% fractile curves, as presented in Fig. 1 (Vamvatsikos and Cornell, 2004a). Additionally, limit-states can be easily defined on the IDA curves (Vamvatsikos and Cornell, 2004a). Immediate Occupancy (IO) is violated when the building exceeds $\theta_{\max} = 2\%$ and Collapse Prevention (CP) is reached when the local slope on the IDA curve is 20% of the elastic slope or $\theta_{\max} = 10\%$, whichever occcurs first (both limit-states defined in FEMA, 2000). Finally, the global dynamic instability (GI) is evident by the characteristic flattening on each IDA, termed the *flatline*, where the structure responds with practically infinite *EDP* to any *IM* increase. Such limit-states can also be summarized into their 16%, 50% and 84% values (Fig. 1). By combining them with Probabilistic Seismic Hazard Analysis within a proper framework (e.g., Cornell et al., 2002; Vamvatsikos and Cornell, 2002), the mean annual frequencies (MAFs) of exceeding each limit-state can be estimated, one of the ultimate goals of PBEE. Still, the calculation of the full, twenty-record IDA for this model requires about 24 hours of computing on a single 1999-era processor, something that may be beyond the practicing engineer.

A path to a simpler solution appears if the SPO of the MDOF system is plotted on $\theta_{\max}$ versus $S_a(T_1, 5\%)$ axes, where the total base shear is divided by the total mass and scaled to match the elastic part of the IDA by an appropriate factor (that is equal to one for SDOF systems). By thus plotting the SPO curve versus the median IDA curve on the same graph (Fig. 2), it is observed that both curves are composed of the same number of corresponding and distinguishable segments (Vamvatsikos and Cornell, 2002). The elastic segment of the SPO coincides by design with the elastic IDA region, having the same *elastic stiffness*, while the yielding and hardening of the SPO (evident by its non-negative slope up to the peak) forces the median IDA to approximately follow the familiar *equal displacement* rule for moderate period structures (Veletsos and Newmark, 1960) by maintaining the same slope as in the elastic region. Past the peak, the SPO's negative stiffness appears as a characteristic flattening of the IDA, the flatline, that eventually signals global collapse when the SPO curve reaches zero strength. This apparent qualitative connection of the SPO and the IDA drives our research effort to provide a simple procedure that will use the (relatively easy-to-obtain) SPO plus some empirical quantitative rules to estimate the fractile IDAs for a given structure, providing the IDA curves at a fraction of the IDA computations.

SPO2IDA for SDOF systems

Based on the established principle of using SDOF oscillators to approximate MDOF systems, the SPO-to-IDA connection has been investigated for simple oscillators. The SDOF systems studied were of short, moderate and long periods with moderately pinching hysteresis and 5% viscous damping, while they featured backbones ranging from simple bilinear to complex quadrilinear with an elastic, a hardening and a negative-stiffness segment plus a final residual plateau that terminated with a drop to zero strength. The oscillators were analyzed through IDA and the resulting curves were summarized into their 16%, 50% and 84% fractile IDA curves which were in turn fitted by flexible parametric equations (Vamvatsikos and Cornell, 2004b). Having compiled the results into the SPO2IDA tool, available online (Vamvatsikos, 2002), an engineer-user is able to effortlessly get an accurate estimate of the performance of virtually any oscillator without having to perform the costly analyses, almost instantaneously recreating the fractile IDAs in normalized coordinates of $R = S_a(T_1, 5\%)/S_a^y(T_1, 5\%)$ (where $S_a^y(T_1, 5\%)$ is

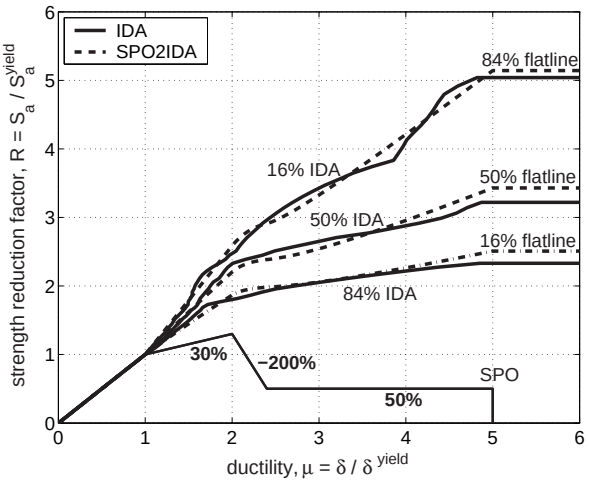

Fig. 3. The 16%, 50% and 84% fractile IDAs for a $T = 0.92$ s oscillator with the displayed backbone, estimated using both IDA and SPO2IDA.

the $S_a(T_1, 5\%)$-value to cause first yield) versus ductility μ.

A typical example of applying SPO2IDA appears in Fig. 3 where the 16%, 50% and 84% fractile IDA curves of a 5%-damped oscillator with moderately pinching hysteresis are estimated using both IDA (for the twenty previously mentioned records) and SPO2IDA. The oscillator's period is $T = 0.92$ s and its backbone has a hardening segment with stiffness 30% of the elastic up to $\mu = 2$, followed by a -200% negative stiffness segment plus a residual plateau that has a strength 50% of the yield strength and ends at $\mu = 5$. The accuracy achieved by SPO2IDA is remarkable everywhere on the IDA curves, even close to collapse. Evidently, SPO2IDA is a uniquely powerful R-μ-T relationship that will provide not only central values (mean and median) but also dispersions of strength reduction R-factor (given μ) and of ductility μ (given R) for oscillators, even beyond the peak of complex backbones.

SPO2IDA for MDOF Systems

Adopting an approach similar to FEMA 273 (FEMA, 1997), the SDOF IDA results generated by SPO2IDA can be used to approximate the seismic behavior of the first-mode-dominated MDOF system. This entails using an SDOF oscillator having the structure's fundamental period, whose backbone closely matches the SPO of the MDOF building. The resulting fractile IDA curves for the SDOF system only need to be properly rescaled from their R, μ coordinates to predict the fractile θ_{roof} IDAs and additionally, using the SPO, can be transformed to estimate the fractile $\theta_{\max}$ IDAs. While the methodology may seem straightforward, the ability of SPO2IDA to extend the results well into the SPO's post-peak region pushes the method to its limits and poses several challenges that have to be overcome.

Defining the SPO

While for an SDOF system the SPO is uniquely defined, this is not the case for the MDOF; depending on the load pattern selection, one may generate several different SPO curves, as evident in Fig. 4. Therein appear the θ_{roof} SPOs for the 9-story building subjected to four

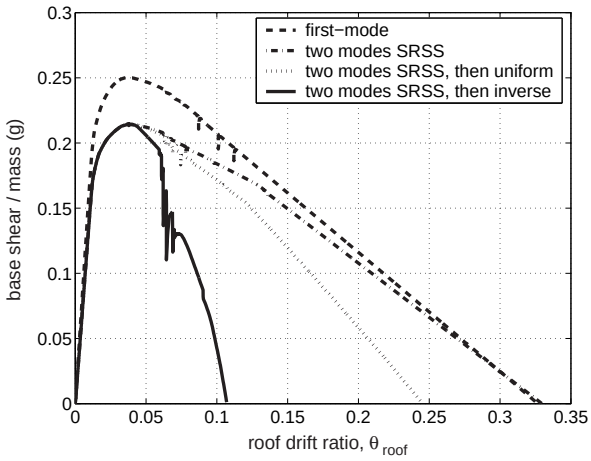

Fig. 4. Four θ_{roof} SPOs produced by different load patterns.

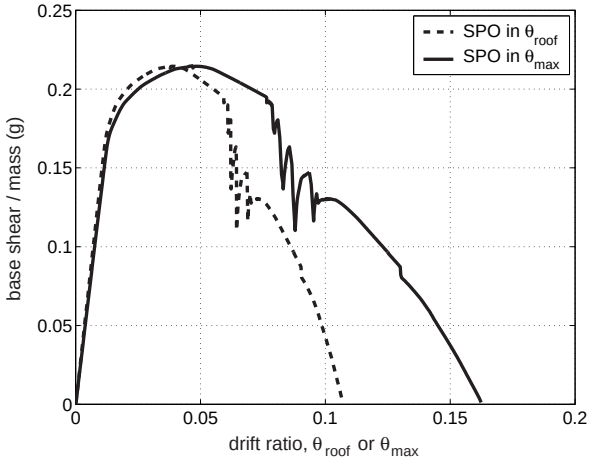

Fig. 5. The most-damaging of the four SPO curves, shown in both θ_{roof} and θ_{max} terms.

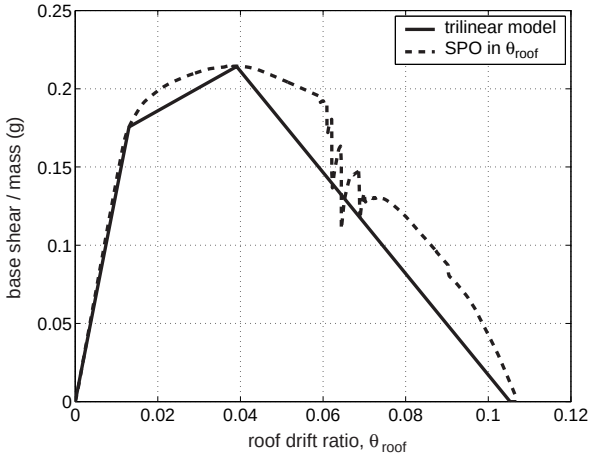

Fig. 6. Approximating the most-damaging of the four θ_{roof} SPO with a trilinear model.

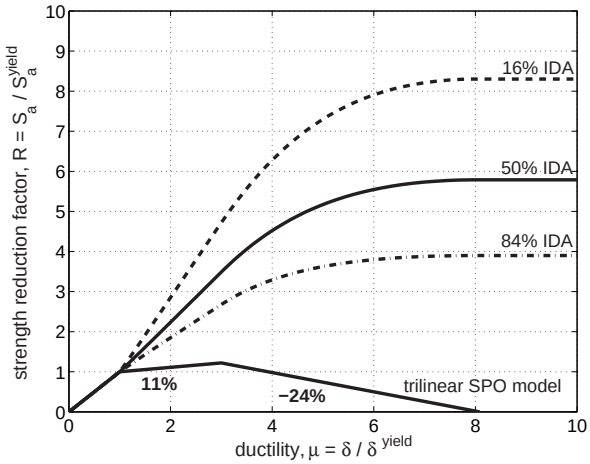

Fig. 7. The fractile IDA curves for the SDOF with the trilinear backbone, as estimated by SPO2IDA.

different load patterns, producing four quite different SPOs. Beginning from the outermost SPO to the innermost, the following can be observed:

1. A load pattern that is proportional to the first-mode shape times the story masses is the most optimistic of the four, as it predicts the highest strength and roof drift ratio, $\theta_{\text{roof}} \approx 0.32$, before system collapse occurs.

2. If, instead of just the first mode, a Square-Root-Sum-of-Squares (SRSS) combination of the first two mode shapes is used the second most optimistic curve is produced, where the maximum strength has dropped significantly but the roof drift ratio at collapse remains $\theta_{\text{roof}} \approx 0.32$.

3. By changing the load pattern at the peak of the previous SPO to a uniform one, i.e., a shape that is directly proportional to the story masses and actually resembles an SRSS of the first two mode shapes of the damaged structure at the peak of the SPO, a severer drop towards collapse is uncovered, with zero-strength occurring at $\theta_{\text{roof}} \approx 0.24$.

4. If, instead of the uniform, the inverse of the pre-peak SRSS pattern (the minimum force now being at the roof-level) is imposed in the post-peak region, it surprisingly produces the severest SPO of all, with global collapse happening at $\theta_{\text{roof}} \approx 0.11$; this is almost one third of the prediction generated by the pure first-mode load pattern.

In essence, the choice of the load pattern has a significant effect on the calculated SPO curve for large levels of deformation and, evidently, each of the four possible realizations pictured in Fig. 4 will produce a different estimate for the seismic demands and capacities. As shown for simple oscillators by Vamvatsikos and Cornell (2004b), by moving from the outermost SPO to the innermost one the estimates of *EDP*-demands past the SPO peak will monotonically increase and, correspondingly, the estimated *IM*-capacity for any limit-state that lies beyond the peak will decrease.

So, how is one to choose among the four SPOs? Since the full IDA results are available the deformed shapes of the structure produced by the various SPOs can be compared versus the IDA. While the median IDA deformed shape shows that in the post-peak region most of the deformations are concentrated on the upper floors, only the innermost (most-damaging) of the four SPOs manages to produce a similar deformation pattern. The other three load patterns seem to concentrate deformations mostly at the lower floors, thus not forcing the structure through the same path to collapse as the dynamic analysis does. It is natural that this most-damaging, worst-case SPO will provide a good approximation to the behavior of the 9-story structure during a nonlinear dynamic analysis.

Such a conclusion can be generalized to structures other than the particular 9-story; it makes sense to assume that a structure under seismic excitation will collapse following the weakest-link, most-damaging, least-energy path. On the other hand, the use of a rigid load pattern will, in general, constrain the deformed shape of the structure, allowing it to withstand higher lateral loads and carry them to higher ductilities. Hence, the SDOF oscillator whose backbone mimics the worst-case SPO will most accurately approximate the dynamic behavior of the true MDOF model. Specifically, it should be expected that in the post-peak region the further an SPO lies from the worst-case one, the more unconservative results it will produce; i.e., SPOs that envelop the worst-case one, when they are used as basis for the calculations of our method, they will generate upper-bound estimates of limit-state capacities and lower-bound estimates of demands. Hence, the focus will be on the most-damaging of the four SPOs and it will be used for all the calculations that follow.

Unfortunately, there is no obvious recipe to find the worst-case SPO. It is hard to predict in advance what load pattern will be the most appropriate, especially if one does not have a priori the dynamic analysis results to confirm that the dynamic and static deformed shapes match. Fully adaptive schemes may prove to be able to find the least-energy path to collapse, several candidates having been proposed at least by Krawinkler and Seneviratna (1998), Gupta and Kunnath (2000) and Antoniou et al. (2002), but none of the proposed schemes has been sufficiently tested and verified in the post-peak region, where good accuracy matters the most for all limit-states that lie close to global dynamic instability (e.g., CP and GI). A simpler, viable solution for regular structures involves using a pattern proportional to the SRSS of several mode shapes times the story masses or a code-supplied pattern, at most up to the peak of the SPO (i.e., $\theta_{\text{roof}} \approx 0.02$ or $\theta_{\max} \approx 0.04$ in Fig. 5), and consequently testing at least three configurations in the post-peak region: Continuing the pre-peak pattern (i.e., maximum force is at the roof), changing to a uniform or using the inverse of the pre-peak pattern (maximum force at the first story). By performing these three basic pushovers a sufficiently broad coverage is obtained and a reasonable load pattern can be picked that will provide a good enough approximation to the overall most damaging, worst-case SPO.

Once there is an acceptable estimate of the worst-case θ_{roof} SPO, it is a simple matter to approximate it with a piecewise-linear backbone, in this case a trilinear elastic-hardening-negative model (Fig. 6), and process it through SPO2IDA. Instantaneously estimates of the

fractile IDAs are obtained (normalized to R and μ) for the SDOF with the matching trilinear backbone, as shown in Fig. 7.

Estimating the IDA elastic stiffness

SPO2IDA will provide accurate estimates of the SDOF system fractile IDAs, but the results will be in dimensionless R versus μ coordinates and need to be properly scaled to $S_a(T_1,5\%)$ versus θ_{roof} or θ_{max} axes. Therefore, it is necessary to determine for each x%-fractile, $x \in \{16,50,84\}$, the values of $S_a(T_1,5\%)$, θ_{roof} and θ_{max} that correspond to its yield point, namely $S^y_{a,x\%}(T_1,5\%)$, $\theta^y_{\text{roof},x\%}$ and $\theta^y_{\text{max},x\%}$. This task is trivial for an SDOF system; the backbone directly provides the yield displacement (same for all fractiles), while it also offers the yield base shear, which when divided by the total mass will result to the value of $S^y_a(T_1,5\%)$ (again, common for all fractiles). This is much harder for an MDOF system, mainly due to the effect of the higher modes; some records will force the structure to yield earlier and some later, at varying levels of *IM* and *EDP*. The problem can be simplified if it is assumed that the SPO accurately captures at least the median value $\theta^y_{\text{roof},50\%}$ and that all fractile IDAs yield at about the same value of $S^y_{a,x\%}(T_1,5\%)$. This assumption is not strictly true for MDOF systems and it becomes highly accurate only if the first mode is dominant but, in general, it is more than enough for our purposes. In this case, the problem comes down to estimating just the elastic stiffness (*IM*/*EDP*) of the median θ_{roof} and θ_{max} IDA, or, even better, the elastic stiffness of all three fractile θ_{roof} and θ_{max} IDAs, $k_{\text{roof},x\%}$ and $k_{\text{max},x\%}$ respectively.

Since such a task involves dynamic linear elastic analysis, it can be easily performed with a minimum of computations. The direct way is to select a suitable suite of records and perform elastic response spectrum or timehistory analysis for each record to determine the θ_{roof} and θ_{max} response. Then, the 16%, 50% and 84% fractiles can be estimated from the sample of elastic θ_{roof} and θ_{max} stiffnesses, $S_a(T_1,5\%)/\theta_{\text{roof}}$ and $S_a(T_1,5\%)/\theta_{\text{max}}$, that have been calculated for each ground motion.

A simpler method involves approximating the median IDA θ_{roof} and θ_{max} elastic stiffness by dividing any elastic SPO level of base shear by the total building mass times the corresponding elastic SPO θ_{roof} or θ_{max} value respectively. This is the same operation one would perform for an SDOF system, hence no information about the variability in the elastic stiffnesses can be recovered. Therefore, one is forced to assume that $k_{\text{roof},x\%} = k_{\text{roof},50\%}$ and $k_{\text{max},x\%} = k_{\text{max},50\%}$, which is accurate only when higher modes are negligible. This is the same assumption adopted for the standard Nonlinear Static Procedure, e.g., Fajfar and Fischinger (1988), Fajfar and Gaspersic (1996), FEMA (1997), although, in that case, normalization is done by the first mode mass rather than the total, something that usually makes very little difference.

Obviously, only the first method is an exact calculation of the elastic IDA stiffnesses, and hence is the method of choice for the calculations to follow. The simpler method reduces the computational load, but in a manner similar to FEMA (1997), it neglects the variability in the elastic stiffness. This reduces its accuracy and restricts its usefulness to shorter buildings with insignificant higher mode effects. Ultimately, the selection of the estimating procedure is a trade-off between speed and accuracy, and depends solely on each user's needs.

Putting it all together

Having determined the appropriate elastic stiffnesses for the fractile IDAs, all that remains is to properly de-normalize and scale the SPO2IDA results, from R versus μ coordinates, into the $S_a(T_1,5\%)$ versus θ_{roof} and θ_{max} axes. Since the SPO has been approximated with a trilinear elastic-hardening-negative model (Fig. 6), its yield-point values of base shear, θ_{roof} and θ_{max}, namely F^y, $\theta^y_{\text{roof,spo}}$ and $\theta^y_{\text{max,spo}}$, are readily available. As explained previously, it is assumed that each x%-fractile IDA, $x \in \{16,50,84\}$, yields at the same value of $S^y_{a,x\%}(T_1,5\%)$, but at different $\theta^y_{\text{roof},x\%}$ and $\theta^y_{\text{max},x\%}$, hence, for all $x \in \{16,50,84\}$:

$$S^y_{a,x\%}(T_1,5\%) = \theta^y_{\text{roof,spo}} \cdot k_{\text{roof},50\%} \tag{1}$$

$$\theta^y_{\text{roof},x\%} = \frac{S^y_{a,x\%}(T_1,5\%)}{k_{\text{roof},x\%}} \tag{2}$$

$$\theta^y_{\text{max},x\%} = \frac{S^y_{a,x\%}(T_1,5\%)}{k_{\text{max},x\%}} \tag{3}$$

Using Eqs (1–3), it becomes trivial to rescale the results of SPO2IDA and bring them in $S_a(T_1,5\%)$ versus θ_{roof} axes to generate the θ_{roof} fractile IDAs, as seen in Fig. 8(a), which clearly compare very well against the real IDAs.

If all that is desired is an estimate of the *IM*-capacity for global dynamic instability of the structure, there is no need to proceed further. On the other hand, to estimate other limit-state capacities (e.g., IO or CP), the IDAs must be expressed in other *EDP*s, usually θ_{max}. The SPO curve actually provides the means for such a transformation thanks to the direct θ_{roof}-to-θ_{max} mapping it establishes when expressed in θ_{roof} and θ_{max} coordinates (Fig. 5), a concept that has been extensively used at least in FEMA 273 (FEMA, 1997). The proposed variation involves shifting the *EDP* axes of the SPO for each x%-fractile, scaling the elastic θ_{roof} values of the SPO by $\theta^y_{\text{roof},x\%}/\theta^y_{\text{roof,spo}}$ and shifting the inelastic θ_{roof} values by $\theta^y_{\text{roof},x\%} - \theta^y_{\text{roof,spo}}$. By performing the equivalent operation to the θ_{max} SPO values, i.e., scaling the elastic θ_{max} by $\theta^y_{\text{max},x\%}/\theta^y_{\text{max,spo}}$ and shifting the inelastic values by $\theta^y_{\text{max},x\%} - \theta^y_{\text{max,spo}}$, a custom θ_{roof}-to-θ_{max} mapping is provided that will correctly transform demands for each fractile, recognizing the variability in elastic stiffness. Of course, were it possible to get the equivalent of a "fractile SPO", by tracing in some way the force-deformation path that the structure would follow for 16%, 50% and 84% of the ground motion records, such transformations would not be needed. In the absence of such data, this method is used to roughly approximate such fractile SPOs.

The results are visible in Fig. 8(b) and compare favorably with the real IDA estimates. Indeed, the estimated IDAs seem to slightly overestimate capacities and underestimate demands, mostly an effect of higher modes plus having just an approximate rather than the real worst-case SPO. For example, the post-peak load pattern cannot take advantage of the sharp drops due to connection fracturing that clearly appear (Fig. 5), but instead allows the structure to recover. A more adaptive pattern would probably do better. Still, even this rough approximation is good enough considering the roughly $\pm$20% standard error (estimated by bootstrapping, Efron and Tibshirani, 1993) that exists in estimating the fractiles from the twenty-record full IDA.

On the other hand, regarding ease-of-computation, if a single 1999-era processor is used the analysis time is reduced from 24 hours for the MDOF IDA to only several minutes for the SPO and the elastic response spectrum analyses, not to mention the practically instantaneous SPO2IDA procedure. Thus, a fast and inexpensive estimate of the MDOF dynamic behavior is achieved at only a small cost in accuracy, the results, at least for this structure, lying within

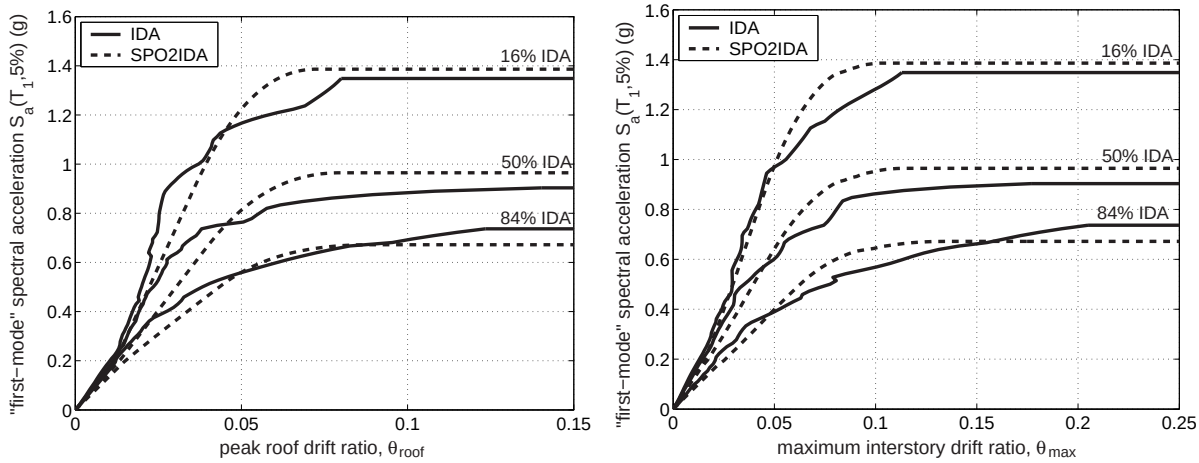

(a) IDA and SPO2IDA estimated θ_{roof} fractile curves (b) IDA and SPO2IDA estimated θ_{max} fractile curves

Fig. 8. Generating the fractile IDAs from nonlinear dynamic analyses versus the MDOF SPO2IDA approximation for the 9-story building.

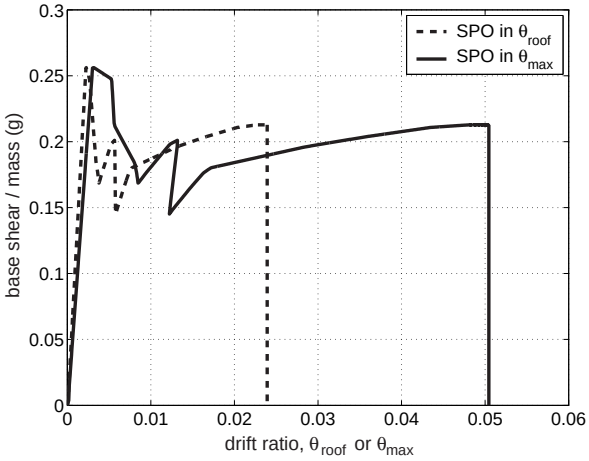

Fig. 9. The most-damaging SPO curve for the 5-story building, shown in both θ_{roof} and θ_{max} terms.

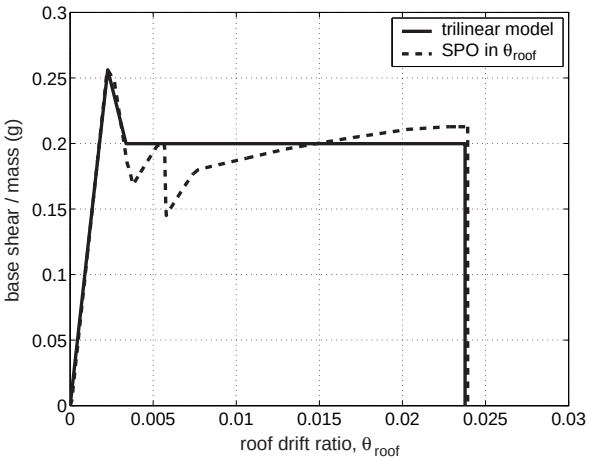

Fig. 10. Approximating the 5-story θ_{roof} SPO with a trilinear model.

the statistical error (caused by the record-to-record variability and limited record suite size) of estimating the fractile IDAs from MDOF nonlinear dynamic analyses with twenty ground motion records.

Application to a 5-story braced frame

To further test the proposed procedure it will be applied to a centerline model of a $T_1 = 1.8$ s, 5-story steel chevron-braced frame with ductile members and connections but realistically buckling braces including P-Δ effects (Bazzurro and Cornell, 1994). For this building, the higher modes are practically insignificant, thus there is little or no ambiguity about the shape of the backbone. It suffices to use a load pattern that is proportional to the first mode shape times the story masses, thus getting the SPO curve shown in Fig. 9 in θ_{roof} and θ_{max} coordinates.

Taking advantage of the SPO2IDA tool, the θ_{roof} SPO curve is closely matched with a trilinear elastic-negative-plateau model (Fig. 10). By combining the results from SPO2IDA with the fractile elastic stiffnesses, the approximate θ_{roof} and θ_{max} fractile IDAs are generated. Using the

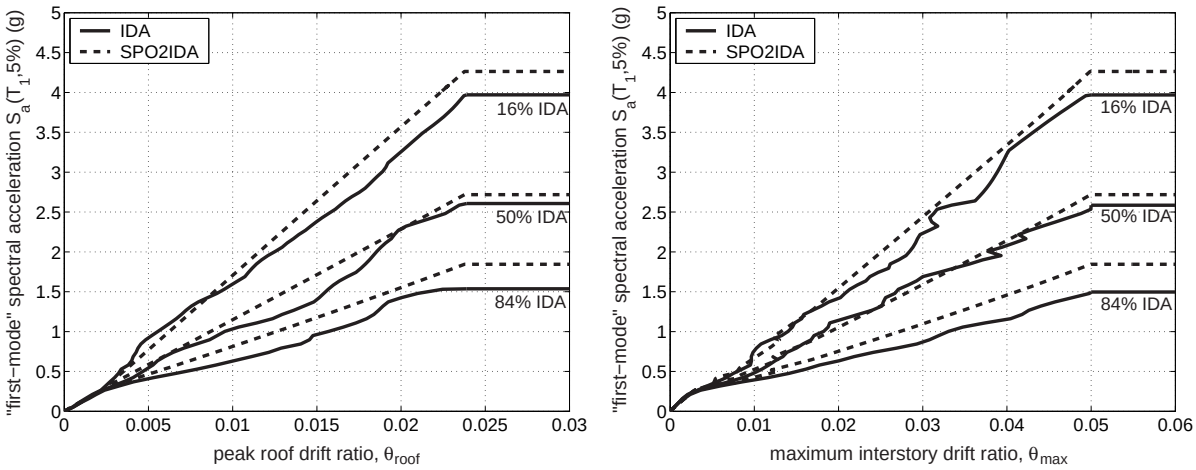

(a) IDA and SPO2IDA estimated θ_{roof} fractile curves (b) IDA and SPO2IDA estimated θ_{max} fractile curves

Fig. 11. Generating the fractile IDAs from nonlinear dynamic analyses versus the MDOF SPO2IDA approximation for the 5-story building.

same suite of records as for the 9-story, the IDA curves are calculated and summarized in their 16%, 50% and 84% fractiles. By comparing the true θ_{roof} fractile IDAs versus the approximate results in Fig. 11(a) it becomes apparent that they are in excellent agreement; the approximate curves certainly lie within the limits set by the estimation error of the twenty-record IDA. Similarly, the θ_{max} fractile IDAs are accurately captured by the approximate results, as shown in Fig. 11(b). Clearly, as expected for such a building with insignificant higher modes, the proposed procedure is a very cost-effective way to approximate the IDA results. But what happens at the other end, for a tall structure with significant higher mode effects?

Application to a 20-story moment frame

In order to test the limits of the method, it will be used on a tall structure, heavily influenced by higher modes. Specifically this is a centerline model of a 20-story steel moment-resisting frame (Luco and Cornell, 2000) with ductile members and connections that includes the influence of the interior gravity columns plus a first-order treatment of global geometric nonlinearities (P-Δ effects). Its first mode has a period of $T_1 = 4$ s and accounts for 80.2% of the total mass, placing this structure beyond the realm of first-mode-dominated buildings. Once more, the structure is analyzed through IDA for the same suite of records used previously, the resulting fractile IDA curves to be used as the standard for comparison.

First of all, the worst-case SPO needs to be determined. Surprisingly, this is an easy task, compared with the previously examined 9-story building. Because of the height of the structure, the massive P-Δ effects are dominating and quickly push the structure towards global collapse. There is only one path to collapse, and almost all reasonable load patterns will force the structure to take it. Hence, a simple load pattern proportional to the first modal shape times the story masses is adequate to capture the worst-case SPO, even beyond its peak, the resulting curve shown in Fig. 12 in θ_{roof} and θ_{max} coordinates. Comparing versus the IDA, it is again confirmed that the worst-case SPO and the IDA produce similar deformation patterns, concentrating most deformation at the lower stories of this building.

Using a trilinear elastic-hardening-negative backbone, the θ_{roof} SPO can be accurately captured (Fig. 13), then SPO2IDA and the fractile elastic stiffnesses can be used to reach the results

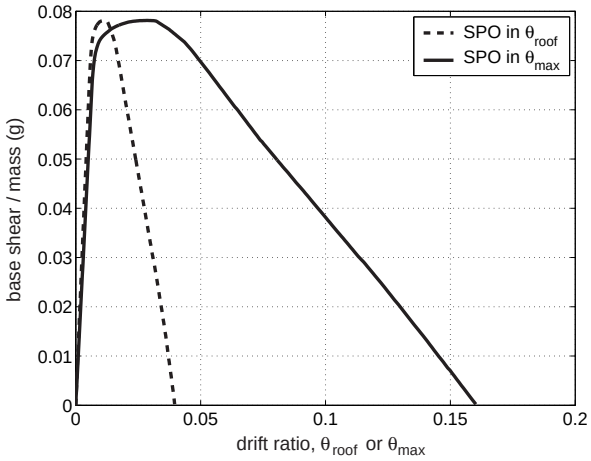

Fig. 12. The most-damaging SPO curve for the 20-story building, shown in both θ_{roof} and $\theta_{\max}$ terms.

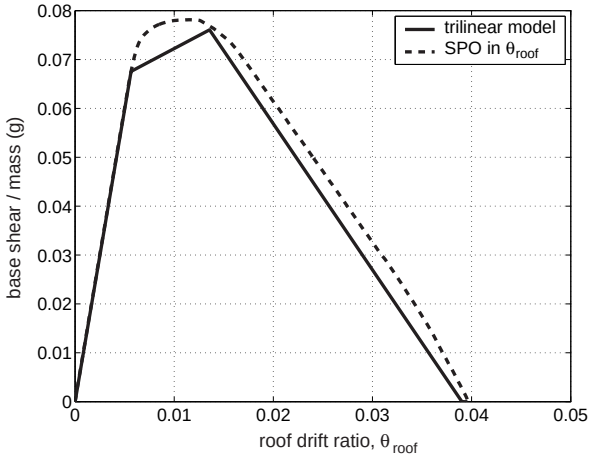

Fig. 13. Approximating the 20-story θ_{roof} SPO with a trilinear model.

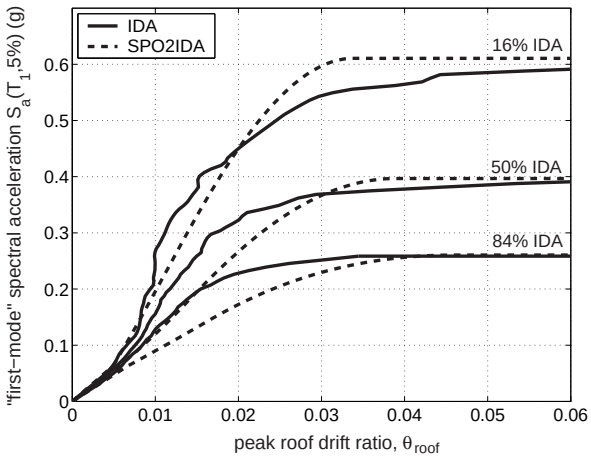

(a) IDA and SPO2IDA estimated θ_{roof} fractile curves

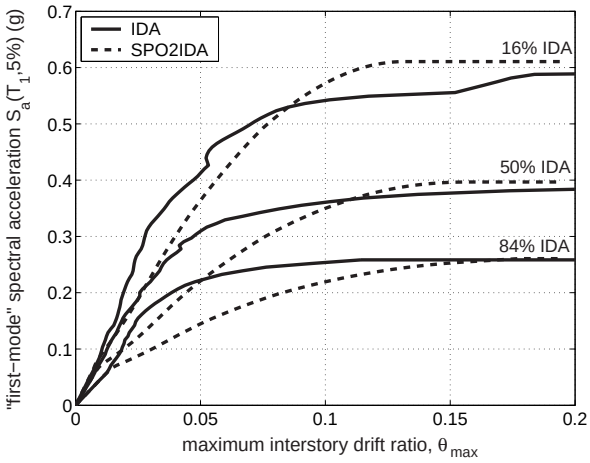

(b) IDA and SPO2IDA estimated $\theta_{\max}$ fractile curves

Fig. 14. Generating the fractile IDAs from nonlinear dynamic analyses versus the MDOF SPO2IDA approximation for the 20-story building.

shown in Fig. 14(a) and 14(b). By comparing them versus the real fractile IDA curves one notices several striking differences and similarities. The θ_{roof} IDAs are relatively well estimated. There is some overestimation of θ_{roof} demands in the near-elastic region, as the MDOF system is capable of high hardening that the SDOF system cannot reproduce, still, in the region near collapse, the θ_{roof} IDAs are almost perfectly matched. On the other hand, the proposed method largely overestimates the $\theta_{\max}$ IDA demands and correspondingly underestimates the $S_a(T_1, 5\%)$-values of capacities, especially for limit-states in the near-elastic domain, but maintains good accuracy close to global collapse. It seems that the higher modes are influencing the accuracy of the approximation, reducing it in the near-elastic range but not close to global collapse.

It is well known that it is very difficult to capture the higher mode effects with just the SPO (Krawinkler and Seneviratna, 1998). The θ_{roof} response is somewhat insensitive to them because of its global nature, but local demand parameters, like $\theta_{\max}$, are not, thus making it very difficult to capture the correct θ_{roof}-to-$\theta_{\max}$ mapping with just the SPO. For example, even in the elastic range, the ratio of the elastic stiffnesses of the median θ_{roof} to the median $\theta_{\max}$ IDA is about 1.5. This means that at any level of $S_a(T_1, 5\%)$, the median $\theta_{\max}$ is about 50%

higher than the median θ_{roof}, i.e., a high degree of deformation localization exists even in the elastic region. On the other hand, the equivalent ratio for the SPO produced with the first-mode load pattern is only 1.3; much less localization is predicted by the static analysis than the dynamic. Even more so, this ratio for the 84% θ_{roof} and $\theta_{\max}$ IDAs is almost 2, which explains why the estimation seems to suffer away from the median in the near-elastic region. Such differences are a direct manifestation of higher modes and cannot be possibly captured by the SPO. This fundamental deficiency of the SPO is precisely the reason why the prediction of the $\theta_{\max}$ fractile IDAs, especially in the near-elastic domain, is not as good for this building. Still, adaptive SPO procedures may better capture the θ_{roof}-to-$\theta_{\max}$ connection, maybe even the variability, and if indeed they are proven to do so, the method described here will highly benefit from their use.

Despite such limitations of the SPO, when nearing global dynamic instability even the elusive $\theta_{\max}$ fractile IDAs are almost perfectly captured. It seems that even such a complex structure can be accurately modeled by an SDOF system close to collapse. While in the elastic or near-elastic region all the modes are interacting to create a complex behavior, as damage accumulates, some of the dominant frequencies seem to be "silenced" and the structure becomes more predictable, more first-"mode" dominated. Some evidence appears if the eigenvalues are calculated from the tangent stiffness matrix at several points along the SPO curve. Then, it is observed that the first-eigenvalue mass steadily increases, from 80.4% of the total mass in elasticity to more than 90.2% at the peak of the SPO. The most probable cause is that the element yielding, buckling or fracturing generates preferred paths of structural deformation, providing locations where most of the deformation concentrates. Thus, the building becomes somewhat less complex, preferring to vibrate in a mode defined by the combination of those damaged elements. It can be suggested that such damage can simplify our structure's behavior and an SDOF system with the proper backbone seems to be able to capture that.

Limit-state capacity estimation using the MDOF SPO2IDA

Apparently, the SPO2IDA approximation provides reasonable estimates, within the limitations of the SPO, for the fractile IDA curves of all three buildings that have been examined. Having these results available one can follow the same steps as done with the full IDA to perform PBEE calculations (Vamvatsikos and Cornell, 2002); the only difference is that the summarized *IM*-capacities have to be calculated for the defined limit-states (IO, CP and GI) directly on the fractile IDAs instead of estimating them individually on each record's IDA curve and then summarizing them (Vamvatsikos and Cornell, 2004a).

This is straightforward for the IO and GI limit-states (Vamvatsikos and Cornell, 2004a); their fractile capacities reside on the fractile IDAs (e.g., Fig. 1) at $\theta_{\max} = 0.02$ and $\theta_{\max} = +\infty$ respectively. Thus, all that is needed is to calculate the values of $S^c_{a,x\%}(T_1, 5\%)$ where each x%-fractile IDA, $x \in \{16, 50, 84\}$, reaches $\theta_{\max} = 0.02$ to violate the IO limit-state, or reaches the flatline for GI. On the other hand, the CP limit-state points (as defined by FEMA, 2000) do not necessarily lie on the fractile IDAs, e.g., Fig. 1, but they are quite close in most cases (Vamvatsikos and Cornell, 2004a). Therefore, it is proposed to apply the SAC/FEMA definition of the CP limit-state point (FEMA, 2000) directly to the fractile IDAs. Thus, each fractile CP capacity point is estimated as the point on the corresponding fractile IDA where the tangent stiffness is 20% of the elastic stiffness or $\theta_{\max} = 10\%$, whichever happens first in $S_a(T_1, 5\%)$-terms. The final results are shown for all three buildings on Table 1.

Table 1. Comparing the real and estimated 16%, 50% and 84% $S_a^c(T_1, 5\%)$ capacities over three limit-states for each of the studied structures. Note that the 5-story reaches global collapse quite early, so the GI and CP limit-states coincide.

		16% (g)		50% (g)		84% (g)	
building	limit-state	Real	Est.	Real	Est.	Real	Est.
5-story	IO	0.61	0.75	1.02	1.05	1.43	1.55
	CP&GI	1.43	1.84	2.23	2.72	4.04	4.26
9-story	IO	0.18	0.14	0.27	0.20	0.33	0.24
	CP	0.57	0.58	0.83	0.88	1.29	1.31
	GI	0.74	0.64	0.91	0.95	1.35	1.37
20-story	IO	0.12	0.08	0.16	0.10	0.21	0.15
	CP	0.23	0.22	0.34	0.35	0.53	0.57
	GI	0.26	0.26	0.39	0.40	0.63	0.61

Note: Est. = Estimated, IO = Immediate Occupancy,
CP = Collapse Prevention, GI = Global Instability

Table 2. Comparing the real and estimated 16%, 50% and 84% $\theta_{\max}$-value of capacity for the CP limit-state for each of the studied structures.

		16%		50%		84%	
building	limit-state	Real	Est.	Real	Est.	Real	Est.
5-story	CP	0.05	0.05	0.05	0.05	0.05	0.05
9-story	CP	0.07	0.10	0.10	0.10	0.10	0.10
20-story	CP	0.05	0.10	0.06	0.10	0.07	0.10

Note: Est. = Estimated, CP = Collapse Prevention,

By comparing the full IDA versus the approximate results in Table 1, it becomes obvious that the proposed method manages to perform very well for a variety of buildings and for each of the three limit-states. Even for the 20-story building, only the IO limit-state is seriously hampered by the approximation, simply an effect of IO happening at the near-elastic region of the IDA where the structure is toughest to predict, as explained earlier. As presented in Vamvatsikos and Cornell (2004a), these *IM*-values are actually all that is needed, coupled with conventional Probabilistic Seismic Hazard Analysis, to get estimates for the MAF of limit-state exceedance. Hence, from the results of Table 1, it is to be expected that the MDOF SPO2IDA method can provide quite accurate MAF predictions.

In order to use an alternative format similar to FEMA 350 (FEMA, 2000), the *EDP*-values of the capacity points are instead needed. For IO the appropriate *EDP*-value is 0.02, by definition, while for GI it is $+\infty$. For the CP limit-state the results are listed in Table 2, where it becomes obvious that the SPO2IDA estimates are quite accurate, except perhaps for the 20-story building. Still, the actual estimate of the MAF of the CP limit-state exceedance will not be as bad as indicated by these results; assuming that the appropriate *EDP*-based integrations are accurately carried through, they should provide the same result with the *IM*-based ones (Jalayer and Cornell, 2002; Vamvatsikos and Cornell, 2004a). These somewhat higher estimates of *EDP* capacity for the 20-story are tempered by equally high estimates of *EDP* demand, in the end producing accurate estimates of MAFs. Using either *EDP* or *IM*-based frameworks, the MDOF SPO2IDA procedure can be used to easily calculate the MAF of exceeding a limit-state. It may even be used for higher-mode influenced buildings if restricted to the near-collapse region.

Sensitivity to user choices

The SPO2IDA method for MDOF structures has proven to be quite accurate. Still, several questions may be raised, regarding the sensitivity of the capacities displayed in Tables 1 and 2 to the average user's choices when applying the proposed methodology.

Obviously, the largest effect comes from finding or missing the right SPO. When the structure fails due to a global failure mode, e.g., due to P-Δ like the 20-story building, or it has insignificant higher mode effects, e.g., like the 5-story building, then the right SPO should be easy to calculate. Almost any reasonable load pattern, e.g., one proportional to the first mode shape times the story masses, will suffice. If, on the other hand, there are significant higher mode effects and the structure fails mainly due to a succession of local events, e.g., connections fracturing or braces buckling, then it is much tougher to find the worst-case SPO. One needs only use the SPO2IDA tool to understand the large influence of the backbone on the IDA (Vamvatsikos and Cornell, 2004b), and realize that no estimation beyond the SPO peak will be accurate without the right SPO. In such cases, it is important to use several, preferably adaptive, load patterns and, in the absence of a proven automated method, use trial and error to select the best of the tried patterns.

Assuming the right θ_{roof}, θ_{max} SPOs have been found, like in our examples, the first must be fitted with a multilinear model. Obviously, there are many trilinear models that could be used instead of the ones in Figs 5, 9 and 12. Would using them change the final results? It is recommended that one becomes familiar with the SPO2IDA tool and understand the influence of the backbone to the SDOF fractile IDAs (Vamvatsikos and Cornell, 2004b). This greatly helps realize the implications of how to best fit the θ_{roof} SPO. For example, the backbone's hardening slope is not as important, while the negative slope greatly influences global collapse. Therefore, care should be exercised to always fit the θ_{roof} SPO better where it matters most to achieve the most accurate results. Even so, the quadrilinear model offered by SPO2IDA allows much flexibility and, as was the case with all three examples, it can capture the shape of the θ_{roof} SPO quite well. Thus, no major differences should be expected in the final results from this source .

Another important issue is the estimation of the elastic stiffness. Up to now the direct estimation from elastic timehistory analysis was used for each record. How much accuracy will one sacrifice by using a simpler method, and what are the implications for the estimates of capacities? Since the normalized SPO2IDA results for the SDOF fractiles are scaled exclusively by the median elastic θ_{roof} stiffness, $k_{\text{roof},50\%}$, its value directly influences the *IM*-estimates of capacity for all limit-states. As a direct effect of Eqs (1)-(3), if all the other $k_{\text{roof},x\%}$, $k_{\text{max},x\%}$ were accurately predicted but $k_{\text{roof},50\%}$ was overestimated or underestimated by α%, a proportional α% overestimation or underestimation will occur for all limit-state capacities. Intuitively, this can be understood by realizing that the value of $k_{\text{roof},50\%}$ determines the scaling of the vertical *IM*-axis for the fractile IDAs. The five other elastic stiffnesses control the scaling of the horizontal *EDP*-axis. Therefore, errors in calculating them have an effect only on limit-states other than GI, as they cannot influence the height of the flatlines. What they do influence is the θ_{roof} and θ_{max} values of the IDAs, thus causing limit-states like IO and CP to appear earlier or later (in *IM*-terms) than normal. Thus, it makes sense to be accurate in the estimates of all $k_{\text{roof},x\%}$ and $k_{\text{max},x\%}$ values.

Keeping these observations in mind, the accuracy of the elastic stiffness estimation methods proposed earlier will be investigated, i.e., the direct timehistory or elastic response spectrum method and the base shear over mass method. Obviously, if higher modes cannot be neglected,

then the direct method is the only one that can be used. It is by far the best way to estimate the variability in the elastic stiffnesses, caused by the higher modes. If, though, higher modes are deemed unimportant or only the median capacities are of interest, the simpler method can be used to get rapid estimates with little computational effort. The estimates $k_{\text{roof},50\%}$ and $k_{\text{max},50\%}$, as obtained by the two methods, are compared in Table 3, where it becomes obvious that the simpler method performs quite well, even for the 20-story building. At most, it overestimates $k_{\text{roof},50\%}$ by 15%, but in the tall structures it misses $k_{\text{max},50\%}$ by almost 30%, something that should be expected as θ_{max} is a local *EDP*, more influenced by the (neglected) higher modes.

Table 3. Comparing the median IDA elastic θ_{roof} and θ_{max} stiffnesses, as estimated by several different methods for the three structures.

	5-story (g)		9-story (g)		20-story (g)	
method	$k_{\text{roof},50\%}$	$k_{\text{max},50\%}$	$k_{\text{roof},50\%}$	$k_{\text{max},50\%}$	$k_{\text{roof},50\%}$	$k_{\text{max},50\%}$
direct	118.2	90.0	12.6	9.7	11.2	7.4
base shear / mass	114.5	84.6	14.2	13.0	12.0	9.9
50% spectrum	118.2	90.0	18.3	3.0	5.6	0.3
“scaled” 50% spectrum	118.2	90.0	18.7	3.0	6.2	0.3

Looking for an intermediate alternative to the above suggested procedures, the estimates for $k_{\text{roof},50\%}$ and $k_{\text{max},50\%}$ are presented for a seemingly reasonable method; elastic spectrum response analysis is performed using the median spectrum of the unscaled suite of records used for IDA. As shown in Table 3, this is not worth the extra calculations as it badly misses the correct values for all but the most first-mode-dominated building. This is to be expected, as the median spectrum does not necessarily provide the median response for true MDOF structures. Even more so, the 16% or 84% spectra will not provide the 16% or 84% response.

To further prove this point, an “improvement” of the above method is used, where all spectra are first scaled to the same $S_a(T_1, 5\%)$-value and then the median spectrum is generated. Again, the results are less than satisfactory for all but the 5-story building, but even then, the base shear over mass approach is much simpler and almost as accurate.

Conclusions

A new method has been presented that can approximate the seismic demands and capacities of first-mode-dominated MDOF structures for their entire range of behavior, from elasticity to global dynamic instability. Based on the Static Pushover (SPO) and building upon software able to accurately predict the Incremental Dynamic Analysis (IDA) curves for SDOF systems, it can estimate, with reasonable accuracy, the fractile IDA curves of first-mode-dominated MDOF systems. Several novel concepts are derived in the process, perhaps the most important being the worst-case, most-damaging SPO. It often needs carefully selected load patterns to emerge, yet it is the worst-case SPO that best captures the path that leads to global collapse, thus allowing accurate prediction of the IDA results. Equally interesting is the apparent “simplification” that occurs in MDOF systems near global collapse. This permits SDOF systems with appropriate backbones to capture the onset of global dynamic instability even for higher-mode-influenced structures. Combining these observations, it is concluded that simply by using the appropriate SPO curve plus, perhaps, a few elastic response spectrum analyses, the engineer-user is able to generate accurate predictions of the seismic behavior of complex MDOF structures within a fraction of the time needed for a full IDA.

Acknowledgements

Financial support for this research was provided by the sponsors of the Reliability of Marine Structures Affiliates Program of Stanford University.

References

Al-Sulaimani, G. J., and Roessett, J. M. (1985). "Design spectra for degrading systems." *J. Struct. Engng*, ASCE, 111(12), 127–136.

Antoniou, S., Pinho, R., and Rovithakis, A. (2002). "Development and verification of a fully adaptive pushover procedure." *Proc. 12th Eur. Conf. Earthq. Engng*, Paper No. 822, 1–10, London, UK.

Bazzurro, P., and Cornell, C. A. (1994). "Seismic hazard analysis for non-linear structures. II: Applications." *J. Struct. Engng*, ASCE, 120(11), 3345–3365.

Cornell, C. A., Jalayer, F., Hamburger, R. O., and Foutch, D. A. (2002). "The probabilistic basis for the 2000 SAC/FEMA steel moment frame guidelines." *J. Struct. Engng*, ASCE, 128(4), 526–533.

Efron, B., and Tibshirani, R. J. (1993). *An Introduction to the Bootstrap*. Chapman & Hall/CRC, New York.

Fajfar, P., and Fischinger, M. (1988). "N2 — a method for non-linear seismic analysis of regular structures." *Proc. 9th World Conf. Earthq. Engng*, 111–116, Tokyo-Kyoto, Japan.

Fajfar, P., and Gaspersic, P. (1996). "The N2 method for the seismic damage analysis for RC buildings." *Earthq. Engng Struct. Dyn.*, 25(1), 23–67.

FEMA (1997). "NEHRP guidelines for the seismic rehabilitation of buildings." *Report No. FEMA-273*, Federal Emergency Management Agency, Washington DC.

FEMA (2000). "Recommended seismic design criteria for new steel moment-frame buildings." *Report No. FEMA-350*, SAC Joint Venture, Federal Emergency Management Agency, Washington DC.

Gupta, B., and Kunnath, S. K. (2000). "Adaptive spectra-based pushover procedure for seismic evaluation of structures." *Earthq. Spectra*, 16(2), 367–391.

Jalayer, F., and Cornell, C. A. (2002). "A technical framework for probability-based demand and capacity factor (DCFD) seismic formats." *Report No. RMS-43*, RMS Program, Stanford University, Stanford, CA.

Krawinkler, H., and Seneviratna, G. D. P. K. (1998). "Pros and cons of a pushover analysis of seismic performance evalation." *Engng Struct.*, 20(4-6), 452–464.

Lee, K., and Foutch, D. A. (2002). "Performance evaluation of new steel frame buildings for seismic loads." *Earthq. Engng Struct. Dyn.*, 31(3), 653–670.

Luco, N., and Cornell, C. A. (2000). "Effects of connection fractures on SMRF seismic drift demands." *J. Struct. Engng*, ASCE, 126, 127–136.

Miranda, E. (2000). "Inelastic displacement ratios for structures on firm sites." *J. Struct. Engng*, ASCE, 126(10), 1150–1159.

Nassar, A. A., and Krawinkler, H. (1991). "Seismic demands for SDOF and MDOF systems." *Report No. 95*, The John A.Blume Earthquake Engineering Center, Stanford University, Stanford, CA.

Vamvatsikos, D. (2002). "SPO2IDA software for short, moderate and long periods." <http://tremble.stanford.edu/nausika/software/spo2ida-allt.xls> (Feb 12th, 2004).

Vamvatsikos, D., and Cornell, C. A. (2002). "Incremental dynamic analysis." *Earthq. Engng Struct. Dyn.*, 31(3), 491–514.

Vamvatsikos, D., and Cornell, C. A. (2004a). "Applied incremental dynamic analysis." *Earthq. Spectra*, 20(2), 1–31.

Vamvatsikos, D., and Cornell, C. A. (2004b). "Direct estimation of the seismic demand and capacity of oscillators with multi-linear static pushovers through incremental dynamic analysis." *Earthq. Engng Struct. Dyn.*, in review.

Veletsos, A. S., and Newmark, N. M. (1960). “Effect of inelastic behavior on the response of simple systems to earthquake motions.” *Proc. 2nd World Conf. Earthq. Engng*, 895–912, Tokyo, Japan.

Notation

The following symbols are used in this paper:

g	=	gravitational constant, 9.81 m/s^2 ;
$k_{\text{max,spo}}$	=	elastic stiffness of the θ_{max} SPO ;
$k_{\text{max},x\%}$	=	elastic stiffness of the θ_{max} x%-fractile IDA ;
$k_{\text{roof,spo}}$	=	elastic stiffness of the θ_{roof} SPO ;
$k_{\text{roof},x\%}$	=	elastic stiffness of the θ_{roof} x%-fractile IDA ;
R	=	strength reduction factor ;
$S_a(T_1, 5\%)$	=	5%-damped first-mode spectral acceleration ;
T_1	=	first-mode period ;
θ_{max}	=	maximum peak interstory drift ratio ;
θ_{roof}	=	peak roof drift ratio ;
μ	=	peak or maximum ductility ;

Superscripts:

c	=	denotes the limit-state capacity value ;
y	=	denotes the value at first-yield of the system ;

Subscripts:

spo	=	denotes the corresponding value for the SPO curve ;
x%	=	denotes the corresponding value of the x%-fractile IDA curve ;